

Preliminary Report on the Recombination Rates of
Hydrogen and Oxygen over Pure and Impure Plutonium
Oxides

Luis Morales, NMT-11

Los Alamos
National Laboratory

*Los Alamos National Laboratory is operated by the University of California
for the United States Department of Energy under contract W-7405-ENG-36.*

Preliminary Report on the Recombination Rates of Hydrogen and Oxygen over Pure and
Impure Plutonium Oxides.

Luis Morales

Los Alamos National Laboratory

Los Alamos, NM 87544

Abstract

The recombination of hydrogen and oxygen has been studied over a 250 °C temperature range in a 2 % H₂/air mixture. Pressure-volume-temperature data and mass spectrometric results were obtained during gas mixture exposure to pure and impure plutonium oxides. The pure oxide was obtained from oxidation of alpha metal. The impure oxide was obtained through the DNFSB 94-1 R & D program's Materials Identification and Surveillance (MIS) project and selected due to its low plutonium content, 29 weight percent. The initial experiments suggest that the oxide surface is an active catalyst for the recombination reaction and also indicate that steady-state gas compositions are reached. The data are consistent with a catalytic chemical reaction at surface sites as opposed to radiolytic formation of radicals in the gas phase. In addition, the recombination rate is dramatically faster than the radiolysis of adsorbed water initially. The rates of water formation were calculated from the pressure-time curves and reported. The implications of this work on the extended storage of materials is discussed. The rate of recombination serves to limit the potential pressure in the container from water radiolysis. With regard to hydrogen-oxygen recombination, radiolysis of water, or the reaction of plutonium oxide with water, an equilibrium state is indicated. Therefore, the pressure reaches a steady-state value which can be calculated from the properties of the materials involved and the pertinent chemical reactions. Both aspects, kinetics and thermodynamics, are required to properly address the long-term storage issues.

Introduction

Long-term, safe storage of excess plutonium bearing materials is required until stabilization and disposal methods are implemented or defined (1). The Department of Energy, DOE, has established a plan to address the stabilization, packing and storage of plutonium bearing materials from around the complex (1). The DOE's standard method, DOE-STD-3013-96 and its proposed revision, for stabilizing pure and impure actinide materials is by calcination in air followed by sealing the material in welded stainless steel containers (2).

The 3013 standard contains an equation that predicts the total pressure build-up in the can over the anticipated storage time of fifty years. Although this equation was meant to model a worst case scenario, to insure pressures would not exceed the strength of the container at the end of 50 years. As a result, concerns about pressure generation in the storage cans, both absolute values and rates, have been raised with regard to rupture and dispersal of nuclear materials (2). Similar issues have been raised about the transportation of these materials around the complex.

The technical basis for the pressure equation given in the 3013 standard has not been fully established. The pressure equation contains two major assumptions, (1) that hydrogen and oxygen generated from radiolysis do not react to form water and (2) that the oxygen generated by radiolysis reacts with the oxide material and does not contribute to the pressure in the container. With regard to the first assumption, if the formation of water from hydrogen and oxygen is important, then the calculated pressures would be dramatically reduced. The formation of water is thermodynamically favored. In addition, the corporate knowledge from shelf-life programs around the complex is that containers do not show signs of extreme pressurization.

The purpose of this work is to provide a stronger technical basis for the 3013 standard by measuring the recombination rates of hydrogen/oxygen mixtures in contact with pure and impure plutonium oxides. The goal of these experiments was to determine whether the rate of recombination is faster than the rate of water radiolysis. This was accomplished by using a calibrated pressure-volume-temperature (PVT) apparatus to measure the recombination rates when the gas mixture was brought into contact with oxide powders whose temperatures range from 50 to 300 C. These conditions were selected in order to rapidly obtain relevant information and to bracket the temperature conditions expected in a typical storage can. In addition, a 2 % H₂/air mixture encompasses scenarios in which the cans are sealed in air.

Experimental

Starting Materials

The gas mixture used in these experiments was obtained from the Los Alamos National Laboratory gas plant. The nominal composition of the gas as ordered was 2 percent hydrogen, 19 percent oxygen, and 79 percent nitrogen. A sample of this mixture was submitted to NMT-1 for analysis by mass spectrometry.

The pure plutonium oxide powder, PMPOX, was obtained by the oxidation of electro-refined alpha phase plutonium metal at 1000 °C. Typically electro-refined metal contains Al, Si, C, Fe, Ni, whose concentrations are each less than 800 ppm. The oxide was characterized by Debye-Scherrer x-ray powder diffraction to insure phase purity and to determine the oxygen to plutonium ratio based on the lattice constant of the material. In addition the surface area of the powder was measured using the BET technique.

The impure plutonium oxide powder, ARF-102-85-295, was obtained from the Materials Identification and Surveillance (MIS) project. The material was canned for shipment at Rocky Flats about 1985 and shipped shortly thereafter and was probably from a molten salt extraction process. Hanford processed much of this type of oxide in the mid 1980's. As part of the MIS project the material was characterized by a variety of

techniques. In addition, inductively coupled plasma mass spectrometry (ICPMS) was employed to determine the major and minor elemental impurities in the powder. The material was selected for this work because the elemental analysis showed that the material contained 18 percent chloride even after calcination to 650 °C and 27 percent Pu. The surface area of this powder was estimated to be 3 m²/gram based on similar materials examined by during the MIS project.

As part of this study, the impure oxide, ARF-102-85-295 which had been previously calcined in air at 650 °C after receipt at Los Alamos, was characterized by x-ray powder diffraction and thermal gravimetric analysis. The material was examined by x-ray powder diffraction using a SCINTAG XDS-2000 diffractometer. The sample was prepared for x-ray diffraction by light grinding with an Al₂O₃ mortar and pestle. A portion of the sample, approximately 50 milligrams, was then loaded on to strip of double-sided tape which was mounted on an epoxy cylinder 1.25 inches in diameter and 1.25 inches tall. The sample and cylinder were then wrapped with plastic film, checked for contamination and then placed into a specially designed sample holder which is mounted on to the goniometer. The correct sample height with respect to the detector-tube zero point plane was set with an external standard. The sample was exposed to nickel filtered copper radiation; the x-ray tube settings were 45 kilovolts and 40 mA. Diffraction data were collected from 25 to 135 degrees in two theta; the scan time was 8 hours.

Another portion of ARF-102-85-295 was analyzed with a Rheometrics model PL-STA 2000 TGA/DSC which provided thermal gravimetric analysis (TGA) over a given temperature regime. Samples of approximately 20 mg. were consistently handled in the following way. Each sample was exposed to room air for a maximum of 15 minutes while that sample was weighed and then loaded into the apparatus. Once the sample was in the apparatus, the sample chamber whose volume is approximately 15 cm², was flushed with oil-free bottled air. The flow rate was 15 ml/ min; the sample chamber was purged for 3 minutes before the experiment was started. These conditions were selected

to closely model the loss on ignition experiments which are routinely performed in the MIS program.

The details of the TGA experiment are as follows. Once the sample chamber was purged, a temperature program was initiated. This program would set the temperature to 25 °C for a three minute isotherm and then ramp the temperature to 1000 °C at a rate of 10 °C/min. During this temperature ramp, the mass of the sample was monitored at a rate of one datum point per second. The experiment concluded when the temperature reached 1000 °C.

Hydrogen-Oxygen Recombination Experiments

Heterogeneous kinetics experiments consisting of pressure-volume-temperature (PVT) measurements were made on closed chemical systems consisting of pure and impure plutonium oxides and a gas mixture with a nominal composition of 2 percent hydrogen, 19 percent oxygen, and 79 percent nitrogen. This gas composition is below the flammable limit, but represents a conceivable scenario in an air-sealed Pu storage container. The measurements were made over a 250 °C range. The PVT apparatus consists of a MKS Baratron gauge and controller connected to a fixed volume vacuum system. Part of that calibrated vacuum system is the furnace which is a gold coated mini-Conflat nipple fitted with a type K thermocouple via a feedthrough. Nickel gaskets are used in the mini-Conflat flanges to achieve the seal. The powdered samples are held in a flat bottomed gold cup which rests on a gold cylinder inside the furnace. The cylinder is of such length that the bottom of the cup is in contact with the thermocouple. The furnace is operated by a Honeywell, model UDC3000, controller which is capable of maintaining a constant temperature to within 0.5 degrees. Two different PVT apparatus, of essentially the same design, were used. The laboratory designations for the systems are PVT2120-1 and PVT2113-1.

In order to calculate the moles of gas introduced into the PVT systems at 50, 100, 200 and 300 °C, a pressure-temperature calibration was performed. Once the furnace temperature achieved the desired value, Ar gas was introduced into the PVT system until

the pressure reading was 581 Torr, approximately atmospheric pressure at Los Alamos. Power to the furnace was then cut and the furnace was allowed to cool to room temperature. The pressure reading at room temperature was then recorded.

A blank run was made to measure the effects of the system on the recombination rate of hydrogen and oxygen. The furnace for PVT2120-1 was allowed to equilibrate to 300 °C after evacuation to 6×10^{-6} Torr. The gas mixture was introduced until the pressure was approximately 580 Torr. The PVT system was then closed, and the pressure was monitored as a function of time.

For the measurements made on PMPOX, a 105 mg. sample was loaded into PVT2120-1; a 106 mg. sample was loaded into PVT2113-1. The same pure oxide sample, PMPOX, was used for multiple runs in each apparatus. The procedure for the experiments was established as follows. Before each run the samples were baked under dynamic vacuum for 24 hours at 350 °C. While still under vacuum, the temperature was set to the desired value via the controller and allowed to equilibrate. The gas mixture was then slowly introduced into the system until the pressure reading was approximately 580 Torr. This operation usually took about two to three minutes. Immediately after the gas introduction, the system was closed and the pressure was monitored as a function of time. Measurements with PVT2120-1 were made at 200 and 300 °C; runs with PVT2113-1 were made at 50 and 100 °C. These experiments were designated as PVT2120-1-200-p2, PVT2120-1-300-p, PVT2113-1-50-p, and PVT2113-1-100-p. Two experiments were done to investigate the effects that heating under dynamic vacuum would have on the measured pressure-time curves. These experiments were designated PVT2120-1-200-p1 and -p2.

For the measurements made on ARF-102-85-295, a 100 mg sample was loaded into PVT2120-1; a 101 mg sample was loaded into PVT2113-1. In these experiments, the samples were pre-treated by heating at 350 °C under dynamic vacuum. Runs were made in PVT2120-1 at 200 °C and in PVT2113-1 at 300 °C following the same procedure used

for the pure oxide. These experiments were designated as PVT2120-1-200-arf and PVT2113-1-300-arf.

In experiments PVT2120-1-200-p2 and PVT2120-1-300-p, the composition of the gas phase was determined by mass spectrometry. For these initial scoping experiments, the gas was sampled at the end of the experiment. This was done by attaching a valved gas bulb to the PVT system. The system was designed so that the bulb could be evacuated and then filled with a small amount of the gas. Usually the pressure drop after gas sampling was approximately 5 to 10 Torr. Quantitative formation of adsorbed water from the hydrogen and oxygen would produce a total pressure drop of approximately 14 Torr.

Results

The results of the mass spectrometric analysis of the starting gas mixture are as follows: H₂, 2.028%; N₂, 78.138%; O₂, 19.795%; Ar, 0.031%; and CO₂, 0.008%. These were the primary gaseous species, note that water was not found. Some fraction of water, whose magnitude is not known, probably adsorbed on to the instrument's inlet manifold which was not heated.

The x-ray powder pattern for the pure oxide, PMPOX, was that of a face centered cubic material with a lattice constant of 5.5044(6) Angstroms. Based on that lattice constant, the O/Pu ratio was calculated to be 1.978 (3). The results indicate that PMPOX is plutonium oxide which is slightly sub-stoichiometric. The surface area of PMPOX was determined to be 4.8 m²/gram. The powder pattern for the impure oxide, ARF-102-365, is shown in Figure 1 and the data are summarized in Table I. The first column of that table reports the angular value of the reflection, the second column gives the calculated d value for the reflection. Columns three through five list the relative intensities, percent intensities, and the peak widths for each reflection. The lattice constant and calculated oxygen to plutonium ratio for the impure oxide are 5.4081(3)

Angstroms and 1.967 respectively (3). The results indicate that the impure oxide is a mixture of PuO_2 , NaCl, KCl, and chromium oxide.

The thermogravimetric analysis for ARF-102-85-295 is shown in Figure 2. The sample experienced an overall mass loss of 13.80 %. The mass loss occurred in distinct steps: between 25 and 200 °C, 2.17 %; between 200 and 800 °C, 2.22 %; and between 800 and 1000 °C, 9.41 %. The mass loss from 25 to 200 °C is attributed to the vaporization of loosely bound water (4). Mass loss from 200 to 800 °C could be attributed to the pyrolysis of hydro-carbon containing materials or the removal of tightly bound water (5). The mass loss between 800 and 1000 °C is due to the vaporization of NaCl and KCl from the sample.

The relationship between the pressure reading at operating temperature and at room temperature was determined in the closed reactor system. The average room temperature pressures at 50, 100, 200, and 300 °C are 552.61, 517.23, 462.64, and 420.35 Torr respectively. These room temperature pressures, used with the starting gas composition and the ideal gas law, provide the basis to calculate the initial gas compositions in the kinetics experiments, the gas composition as a function of time, and the rate of water formation for each experiment.

In experiments PVT2120-1-200-p1 and PVT2120-1-200-p2, the effect of sample bakeout on the recombination rate was investigated. As previously described, the pure oxide, without any pretreatment, was allowed to react with the starting gas mixture at 200 °C. When that phase of the experiment was complete, that same sample was then baked at 350 °C under dynamic vacuum for 24 hours and then allowed to react again at 200 °C with fresh starting gas. The results of this experiment are shown in Figure 3.

The measured kinetic data, which consist of monitoring the total system pressure as a function of time, are presented in Figure 4 for the pure oxide, PMPOX. Figure 5 gives the comparison between the kinetic data for the pure oxide, on a time scale of 0 to 600 minutes, with the kinetic data for the impure oxide, ARF-102-85-295, collected at 200 and 300 °C. Figure 5a shows the kinetic data in terms of moles of hydrogen

consumed. For each experiment, Table II gives the total pressure at room temperature. These values are the pressure calibration data given previously. Table II also lists the total moles of gas in the system at time zero. These values were calculated from the ideal gas law using the pressures in column three, a temperature of 295 K, and a system volume of 36 cm³. The raw data points for each of the kinetic experiments are listed in Tables IV through VII. The first column gives the measurement time in minutes. The second column reports the total pressure as a function of time. Further description of the contents are provided in the derived results section.

These kinetic data show that the rates at the higher temperatures, 100, 200, and 300 °C, for the pure oxide are essentially the same based on the initial slopes of the pressure-time curves. Only the data collected at 50 °C show deviation from this behavior. Interestingly the data collected at 300 °C for the pure oxide show an upturn after approximately 1000 minutes into the experiment. The data for the 100 °C run for the pure oxide clearly show a sharp break in the slope approximately 100 minutes into the experiment. The blank experiment, performed at 300 °C, shows a slow pressure decrease with time. The decrease in pressure may be attributed to hydrogen reacting with the Ni gaskets. Figure 5 shows that the pressure-time curves for the impure oxide experiments yield rates that are lower than those for the pure oxide counterparts at equivalent temperatures. The calculated rates for each experimental run are summarized and described in the derived results section.

During experiments PVT2120-1-200-P2 and PVT2120-1-300-P on the pure oxides, the gas was sampled at the beginning and end of these experiments for mass spectrometric analysis. Table III reports the gas phase compositions that were determined. Column one identifies the experiment. The second and third columns report the initial and final gas phase compositions respectively. The last column provides the change in the gas composition as a result of interaction with the oxide powder. The results show that roughly stoichiometric amounts of hydrogen and oxygen were consumed to make water. Minor amounts of oxygen were also consumed to make carbon

dioxide, and approximately 0.4 % of the oxygen reacted with some other unidentified “sink”. Stoichiometric amounts of water vapor were not observed in either of the final gas compositions. We attribute this observation to water adsorbing on the inner walls of the PVT system or on the surface of the oxide itself (6).

Derived Results

The following is a brief description of the methodology employed (1) to calculate the rates of hydrogen consumption and water formation from the raw data and (2) to use these rates in a simple analysis of the reaction kinetics. The derived results are summarized following this description. The model used to describe this system is the recombination of hydrogen and oxygen to form water. For every mole of hydrogen consumed a mole of water is produced. The absolute values of these rates are equal but the values of the rates have opposite signs. Based on the calculated initial gas composition and the assumption that hydrogen and oxygen were reacting to form water, the number of moles of hydrogen and oxygen were calculated as a function of time.

Based on the method of initial slopes, the rate of water formation was calculated; a single rate value was calculated from a combination of the 100, 200, and 300 °C data for the pure oxide since the initial slopes of the pressure-time curves were essentially identical. The rate was also calculated at 50 °C for the pure oxide and at 200 and 300 °C for the impure oxide. The units of the rate of water formation are moles H₂O/m² day. Since nominally equal amounts of the pure oxide were used, a total surface area of 0.509 m² was used based on the mass of powder and a measured surface area of 4.8m²/g. The surface area of the impure oxide was estimated to be 3 m²/gram to give a total surface area of 0.303 m².

A general method has been developed (7) to determine the overall reaction order and the rate constant in heterogeneous systems. The following equations are fit to the data:

$$t/p = (nt/2) + 1/K, \text{ given} \quad (1)$$

$$K = kc_0(n-1) \text{ and} \quad (2)$$

$$p = 1 - (c/c_0) \quad (3)$$

where t is the time, p is the fraction reacted, n is the overall reaction order, k is the rate constant, c_0 is the initial concentration of a reactant, and c is the concentration at time, t . A plot of t/p against t should be a straight line with a slope of $n/2$ and an intercept of $1/K$.

For the experiments on the pure oxide, the data are summarized in Tables IV through VII. The first column reports the total pressure in the PVT system. The second column lists the elapsed time in minutes. The third column gives the change in total pressure as a function of time. Columns four and five show the calculated amounts of hydrogen and oxygen used, in Torr, as the experiments progress. These values are based on the assumption that hydrogen and oxygen react to form water. Columns six and seven report the calculated number of moles of hydrogen and oxygen as function of time. Column eight gives the calculated ratio of c to c_0 . The penultimate column reports the fraction of hydrogen reacted, p . The last column provides the quotient t/p . The overall reaction order for the 200 and 300 °C runs was two. The overall order for the 50 and 100 °C runs was four and three respectively. The plot of t/p against t is shown in Figure 6.

For the experiments on the impure oxide, the data are summarized in Table VIII. The first column reports the total pressure in the PVT system. The second column lists the elapsed time in minutes. The third column gives the change in total pressure as a function of time. Columns four and five show the calculated amounts of hydrogen and oxygen used, in Torr, as the experiments progresses. These values are based on the

assumption that hydrogen and oxygen react to form water. Columns six and seven report the calculated number of moles of hydrogen and oxygen as function of time.

From the data in Tables IV through VIII, the rate of water formation was calculated based on the method of initial slopes. As described previously, the data from the 100, 200, and 300 °C runs on the pure oxide were averaged to calculate one rate. Table IX summarizes these calculations and provides the data points used in the least squares fits. Column one of Table IX identifies the temperature and the particular experiment and or experiments. Columns two and three contain the time and calculated moles of hydrogen respectively. These are the data, obtained from Tables IV through VIII described above, that were used in the least squares fit which provided the slope. Each point was weighted equally in the least squares fitting. Column four lists the temperature of the experiment. Column five reports the calculated rate of hydrogen consumption in moles H₂/ min. Column six gives the calculated rate of water production with the following units: moles H₂O/ m² day. Column seven lists the reciprocal temperature in K and column eight gives the natural logarithm of the rate of water formation. The data in columns six and seven for the pure oxide are plotted in Figure 7.

Discussion

The results for the experiments with PMPOX indicate that hydrogen and oxygen combine to form water in the presence of the pure plutonium oxide. In each experiment, the total pressure decreased rapidly after the reactants were combined. The mass spectrometric results for experiments PVT2120-1-300-p and PVT2120-1-200-p2 which were carried out at 200 and 300 °C respectively, show an overall depletion of stoichiometric amounts of hydrogen and oxygen. The mass balances for the mass spectrometric results are in excellent agreement with the assertion that hydrogen and oxygen recombine quickly to form water. As expected, quantitative amounts of water vapor were not observed in either of the final gas compositions. This is attributed to the

absorption of water on the surface of the oxide or the inner walls of the PVT system. The mass spectrometric results also point to the role played by the oxide surface. A small amount of oxygen may have reacted with the oxide powder. In fact, the pure oxide starting material was shown to be sub-stoichiometric by x-ray powder diffraction.

The kinetic results summarized in Figures 4 and 5 indicate that the surface of the plutonium oxide powder plays an important role in the recombination of hydrogen and oxygen. The data collected at 200 °C before and after the thermal/vacuum treatment described in the experimental section show a marked difference in the pressure-time curves and therefore the rate of recombination. The abrupt change in the slope of the pressure-time curve and therefore the rates of recombination at 100 °C suggest that the surface of the oxide plays a role in the recombination of hydrogen and oxygen at this lower temperature as well. For those data the slope, and hence the rate, of the pressure-time curve changes abruptly within 20 minutes. A similar effect, although not as pronounced, is also seen in the pressure-time curve measured at 50 °C. In contrast, the data collected at 200 and 300 °C show a smooth decrease in the pressure with time out to approximately 800 minutes when essentially all the hydrogen had been depleted. These observations are confirmed by the kinetic analysis of the data on the pure oxide. Above 100 °C, the reaction is second order overall. At and below 100 °C, the process may be higher order. It is important to note that the change in the reaction order across the 100 °C temperature boundary is significant.

These data suggest that the concentration of active surface catalytic sites governs the kinetics of recombination early on, and as the reaction proceeds, certain moieties (OH or H₂O for example) occupy these active surface sites thereby reducing the rate of recombination. Above 100 °C, enough thermal energy is delivered to the oxide powder so that a larger fraction of these active sites remain free to catalyze the recombination of hydrogen and oxygen.

The implication is that the recombination reaction is a chemical one involving heterogeneous surface catalysis and is not strongly driven by the radiolytic formation of

radicals in the gas phase under these experimental conditions. Radiolytic processes may be involved to a lesser extent in that the alpha radiation may initiate or enhance the surface reaction. (8) Further work in which the isotopic composition of the oxide and hence the flux of alpha particles is changed, (Pu 239 vs. Pu 242), is needed to resolve this issue.

These initial experiments were designed to provide some initial insight into the mechanistic details but did not provide enough information to distinguish between the Langmuir-Hinshelwood or Eley-Rideal mechanisms for surface catalyzed reactions. For the Langmuir-Hinshelwood mechanism, the rate is proportional to the fractions of two different molecules adsorbed on the surface. If the concentration of one is fixed and the concentration of the other is varied, the rate initially increases, then passes through a maximum, and then steadily decreases. For the Eley-Rideal mechanism, as the concentration of one species is fixed and the concentration of the other is varied, the rate initially increases and then remains constant. In order to distinguish between these mechanisms, one needs to determine whether the rate decreases as the concentration of hydrogen is increased. Future work in which the concentrations of hydrogen and oxygen can be independently varied should help resolve this issue and elucidate the role that the oxide surface plays in the recombination reaction.

The kinetic data indicate that a steady state pressure would be achieved if the experiments were allowed to continue. This statement is largely substantiated by the data collected on the pure oxide at 100 and 50 °C which indicate that these pressure-time curves are tending toward a steady state total pressure. The pressure-time curves obtained from the impure oxide also support this assertion. The steady state gas composition is calculated to be approximately 1% hydrogen.

The implication of these data is that initially surface catalyzed hydrogen/oxygen recombination is the primary process responsible for pressure reduction and/or hydrogen removal from the experimental system. Radiolytic or catalytic decomposition of water would increase the total pressure in the system via the formation of hydrogen and oxygen.

The establishment of a steady-state gas composition would indicate that these rates equalize. The kinetic data collected thus far, indicate this interplay between surface catalyzed recombination and adsorbed water radiolysis.

An possible explanation for the upturn in the data collected at 300 °C for the pure oxide is that the water formed on the surface reacts with the oxide to produce PuO_{2+x} and hydrogen gas. Previous experiments in a study of the reaction of PuO_2 with water at 200 to 350 °C have produced oxide products with compositions up to $\text{PuO}_{2.2}$ (9). The rates of hydrogen generation as a function of temperature were used to calculate an activation energy of 9.7 kcal/ mol in this previous work (9).

The implication of the oxide/ water reaction to the storage issue is that water catalyzes the oxidation of PuO_2 which liberates hydrogen. Two cases are important. If the gas phase contains oxygen, the recombination reaction will form water. The reaction of water and PuO_2 will continue until the equilibrium composition of PuO_{2+x} at a given temperature and hydrogen pressure is reached. If there is no oxygen in the gas phase to react with the hydrogen, then the gas phase is enriched with hydrogen. Again, this process will continue until the equilibrium composition of PuO_{2+x} at a given temperature and hydrogen pressure is reached or until the water, if it is the limiting reagent, is consumed. The important fact relevant to the storage issue is that an equilibrium state is reached. This is likely the reason that high pressures of hydrogen have not been observed in the shelf-life programs. Future experiments will address this issue by the use of real-time mass spectrometry to identify the gaseous species as the equilibrium gas composition is established.

Conclusions

Our preliminary data show that when this gas mixture is exposed to pure plutonium oxide heated above 100 °C, the recombination rate is dramatically faster than the radiolysis of water initially. Under our experimental conditions, the data are more consistent with a chemical reaction of H_2 and O_2 at catalytic sites on the plutonium oxide,

as opposed to radiolytic formation of radicals in the gas phase. Surface catalyzed formation of water on stainless steel and inorganic salts are well known (10, 11). However, radiolysis may be involved to a lesser extent in that the radiation may initiate or enhance the surface reaction. Radiation induced H₂/O₂ gas reactions are well known (8).

Above 100 °C enough thermal energy is provided to maintain a larger fraction of the active sites available for recombination. Below 100 °C, the recombination rate seems to be governed by the number of available sites and the rate at which they are filled. The sharp break in the 100 °C pressure-time curve shows how dramatically the recombination rate is reduced when the active sites become blocked. This type of behavior would not be expected for a recombination reaction dominated by radiolytic formation of radicals in the gas phase. Although the data presented in this report do not allow one to elucidate a mechanism, the role of active surface sites in the recombination reaction has been demonstrated. In the storage environment the temperature may reach above 100 °C, so that the active sites do not remain blocked.

The results of these kinetic experiments suggest that a steady-state gas composition is reached indicating that the rates of recombination and water radiolysis become equal. For this particular initial gas mixture (2 % H₂/air at 580 Torr), the steady-state composition is calculated to be below the flammable limit. Based on these preliminary results, pressurization of sealed containers due to the radiolysis of water adsorbed on the plutonium oxide and/or the water reaction with PuO₂ will be severely limited. This conclusion agrees with the corporate knowledge from shelf-life programs around the complex that plutonium oxide storage containers do not show signs of extreme pressurization.

With regard to hydrogen-oxygen recombination, radiolysis of water, or the reaction of oxide with water, the important fact relevant to the storage issue is that the pressure reaches a steady-state value. That value can be calculated if one knows the properties of the materials involved and the pertinent chemical reactions. Kinetic and thermodynamic information are required to properly address the long-term storage issues.

Future Work

These initial experiments suggest that the oxide surface plays a significant role in the recombination reaction and indicate that a steady-state gas composition is reached. Further work should be directed towards (1) the characterization of the equilibrium gas composition as a function of temperature and initial gas composition, and (2) understanding the mechanism of the recombination reaction especially with respect to radiolytic radical formation as opposed to surface catalysis.

Reaching a thermodynamic steady-state and the characterization of the gas phase composition is of utmost importance. Taken together with even a basic understanding of the chemistry and kinetics involved, the issue of gas generation in the plutonium storage containers could be set in a proper prospective. Incorporation of the recombination rates, water radiolysis rates, and the oxide/water reaction rates into an overall model would allow one to more accurately predict absolute pressures and pressure generation rates over the 50 year design storage life of a container.

Careful experiments in which the initial concentrations of hydrogen and oxygen, surface area, and isotopic composition are varied should provide the information needed to elucidate the mechanism of recombination and the role of the surface as opposed to radiolytic formation of radicals in the gas phase. Experiments using surface science techniques, such as photoelectron spectroscopy, will be initiated to study the interactions of H₂/O₂ mixtures and water on the surfaces of clean plutonium oxide layers. Work needs to be focused on studying the recombination rate from room temperature to 250 °C; it is in that temperature regime that data are lacking and the greatest transition in reaction rates are seen.

Acknowledgment:

This work was supported by the Environmental Management Nuclear Materials Stewardship Program, United States Department of Energy.

References

1. "Assessment of Plutonium Storage Safety Issues at Department of Energy Facilities," US DOE Report DOE/DP/0123T, US Department of Energy, Washington, D.C., 1994.
2. "Criteria for Preparing and Packaging Plutonium Metals and Oxides for Long-term Storage," Department of Energy, DOE-STD-3013-96, September, 1996.
3. E. Garder, T. Markin and R. Street, *J. Inorg. Nucl. Chem.*, 27, pp. 541-551, (1965).
4. "Plutonium Dioxide Storage: Conditions for Preparation and Handling," J. Haschke and T. Ricketts, LA-12999-MS, August, 1995.
5. "Conditions and Results from Thermal Stabilization of Pure and Impure Plutonium Oxides for Long-Term Storage at Department of Energy Sites", Craig S. Leasure, David R. Horrell, and Richard E. Mason, LA-UR-98-3526, September, 1998.
6. "Interactions of Plutonium Dioxide with Water and Oxygen-Hydrogen Mixtures," J. Haschke and T. Allen, LA-13537-MS, January, 1999.
7. J. Moore and R. Pearson, "Kinetics and Mechanism," 3rd edition, John Wiley and Sons, New York, pg. 21, (1981).
8. "Literature Search on Hydrogen/Oxygen Recombination and Generation in Plutonium Storage Environments", J. Lloyd, L. Hyder, and P. Gary Eller, LA-UR-98-4557, January 1999.
9. L. Morales and J. Hascke, "Investigation of the Plutonium Oxide-Water Reaction," Final Programme and Abstracts, Actinides '97 International Conference, Baden-Baden, Germany, September 21-26, 1997.
10. J. C. Beavis, *J. Vac. Sci. Technol.*, 10, p. 386, (1973).
11. "Hydrogen/Oxygen Recombination Rates in 3013-Type Environments: An Interim Report on the Rate of Loss of Hydrogen in Dry Air from Cells Containing Non-Radiolytic Samples", G. Quigley, LA-UR-98-4864.

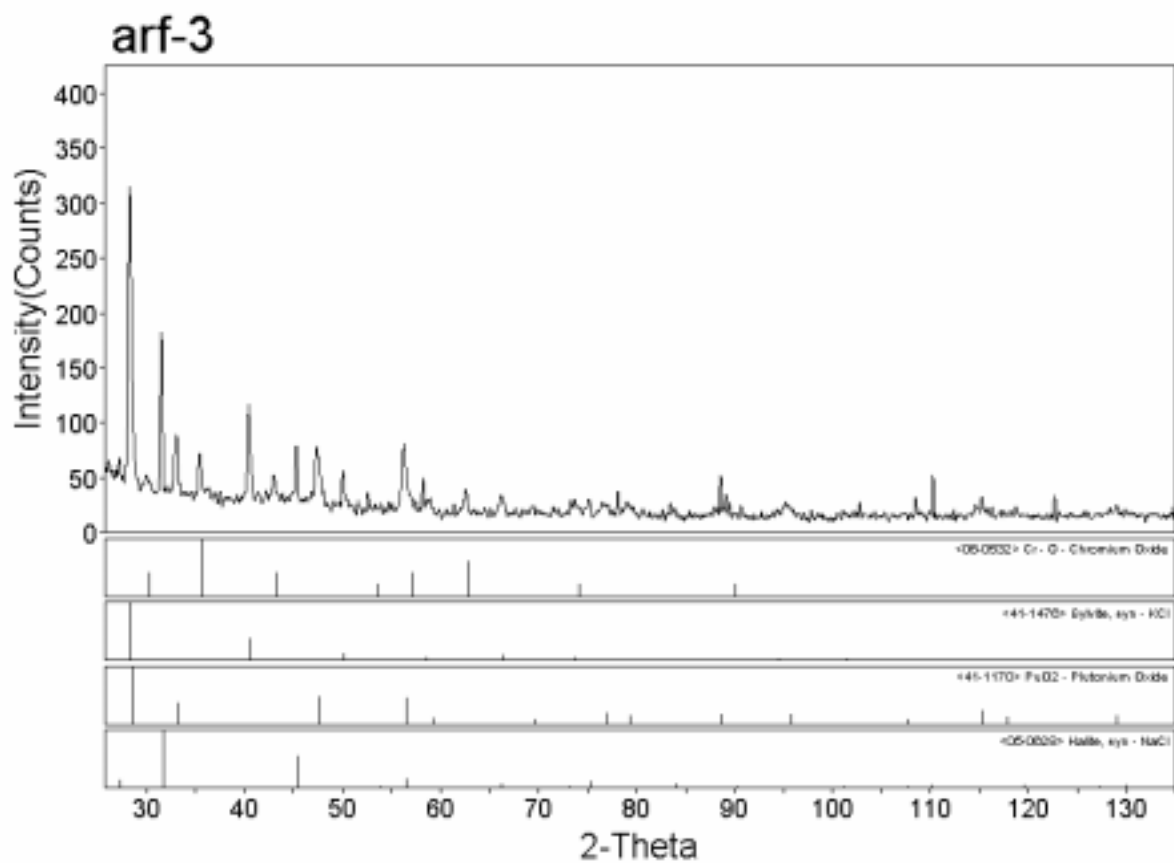


Figure 1. X-ray powder diffraction pattern for ARF-102-85-295. This material had been previously calcined in air at 650 °C.

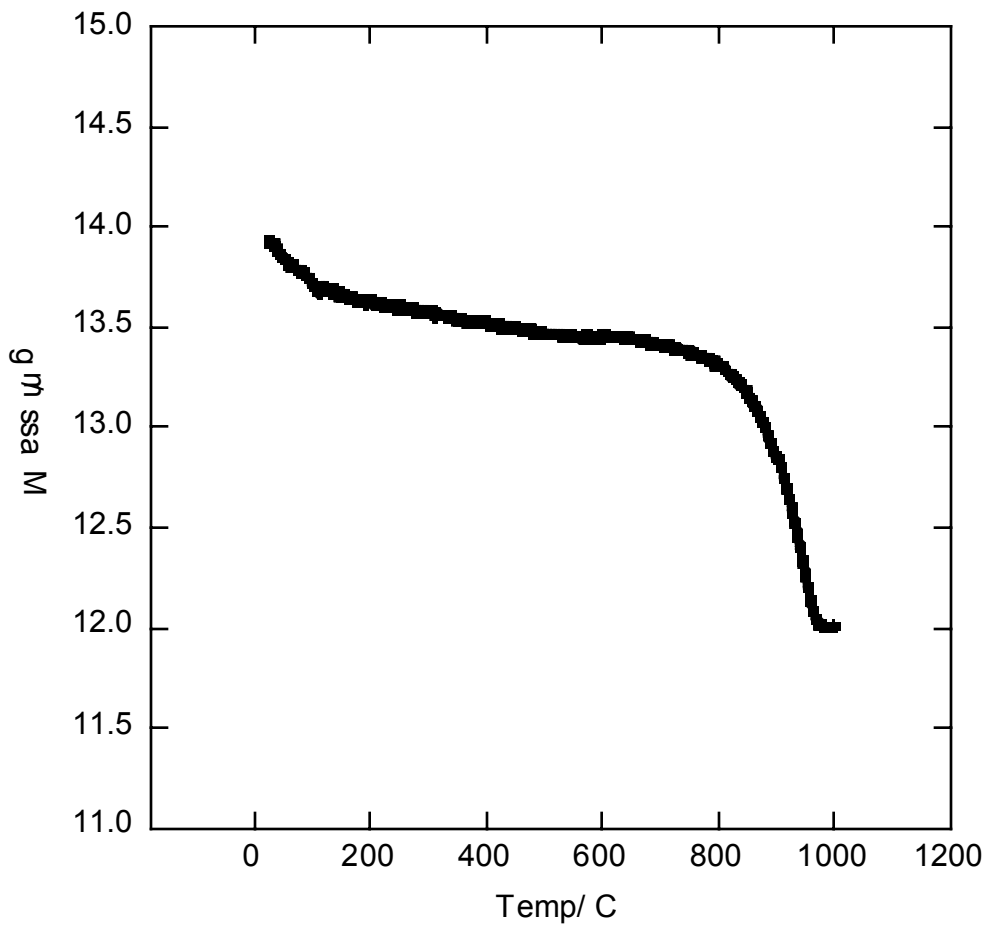


Figure 2. Thermogravimetric analysis (TGA) of a portion of ARF-102-85-295 performed in air with a ramp rate of 10 °C/ min.

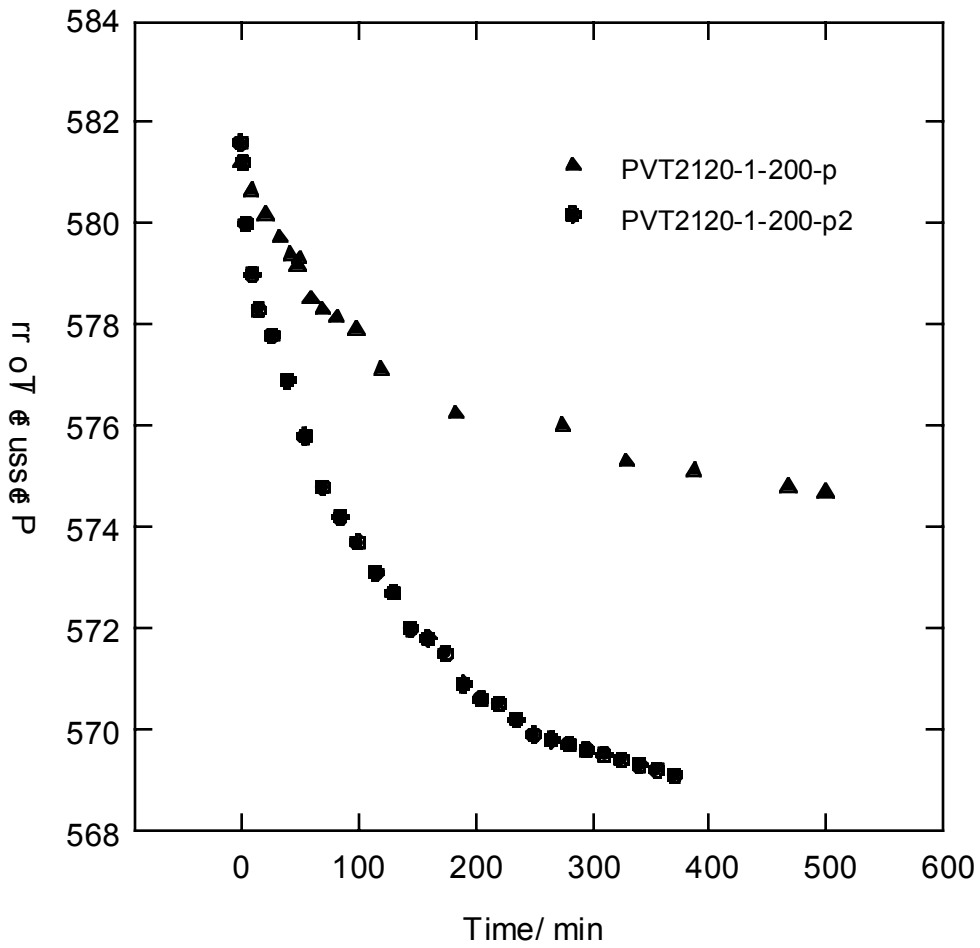


Figure 3. Pressure-time curves obtained at 200 °C for the pure oxide showing the effects that heating under dynamic vacuum have on the reaction rate. In experiment PVT2120-1-200-p the sample was not pre-treated.

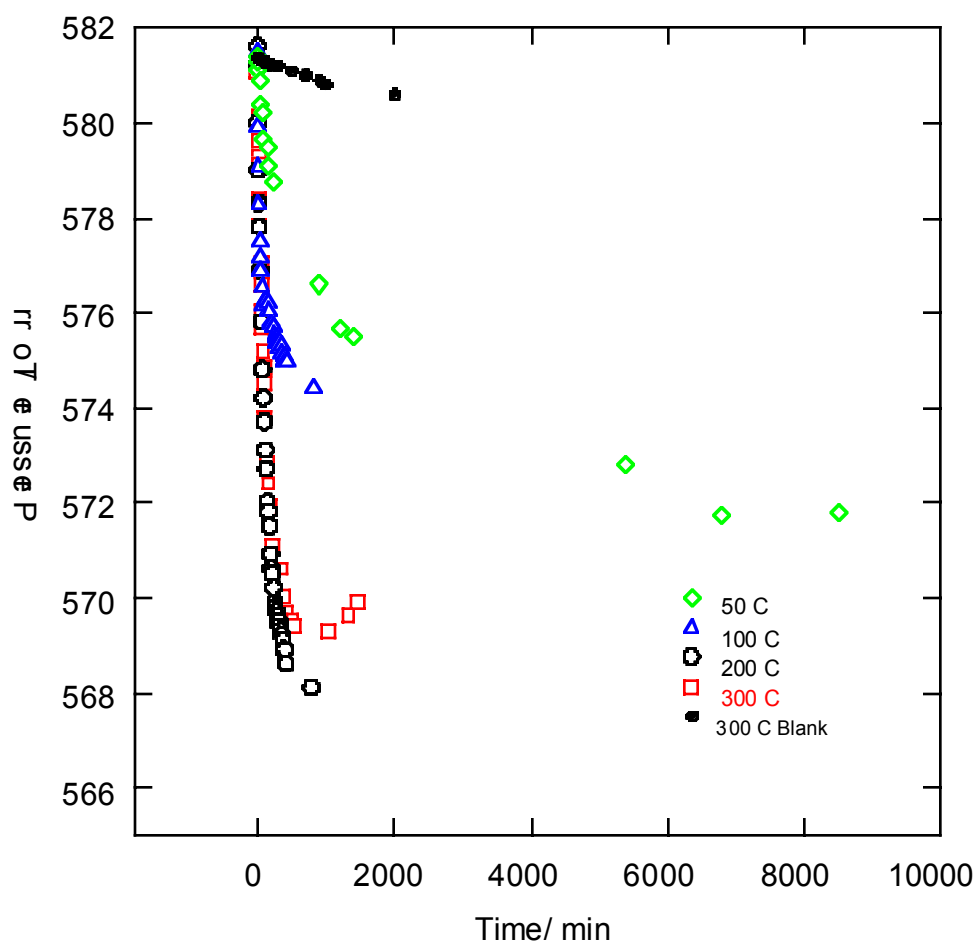


Figure 4. Plots of the pressure-time curves measured for the pure oxide, PMPOX.

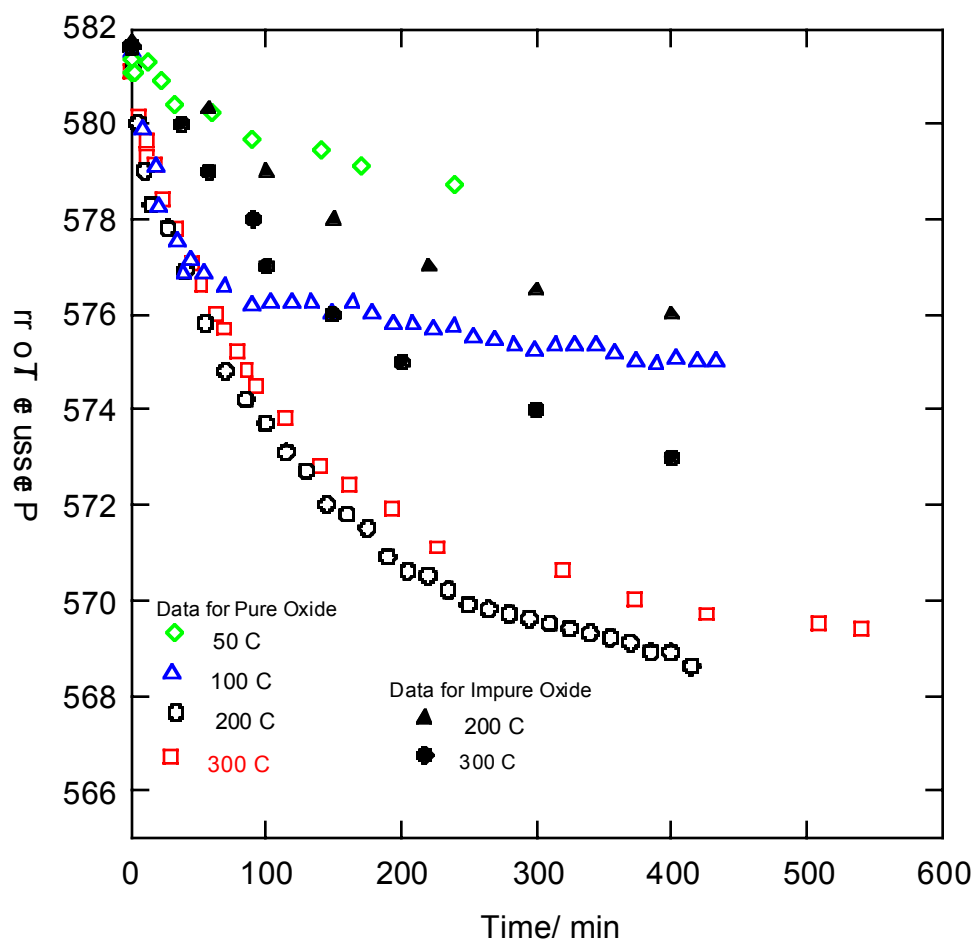


Figure 5. Plots of the pressure-time curves measured for both the pure and impure oxides. A finer time scale is employed to show the details of the data collected early in the experiments. The data for the pure oxide are the same as shown in Figure 4.

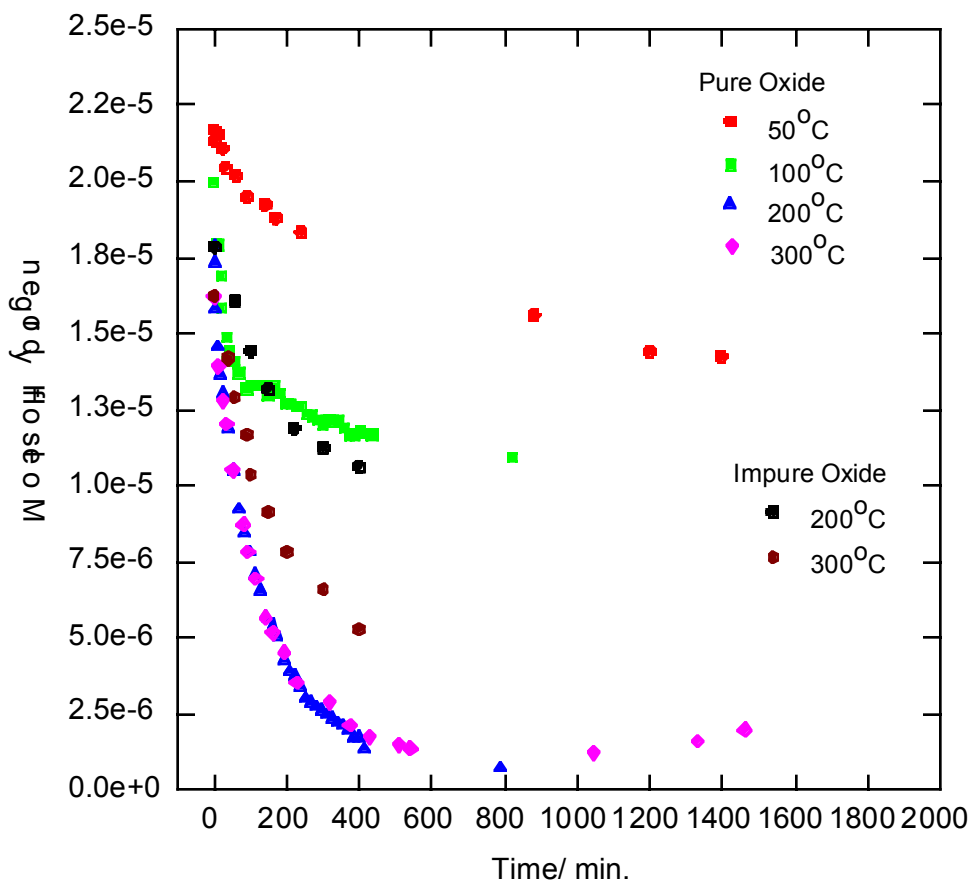


Figure 5a. Plots of the pressure-time curves measured for both the pure and impure oxides as a function of moles of hydrogen consumed during the experiments. A finer time scale is employed to show the details of the data collected early in the experiments. The data for the pure oxide are the same as shown in Figure 4.

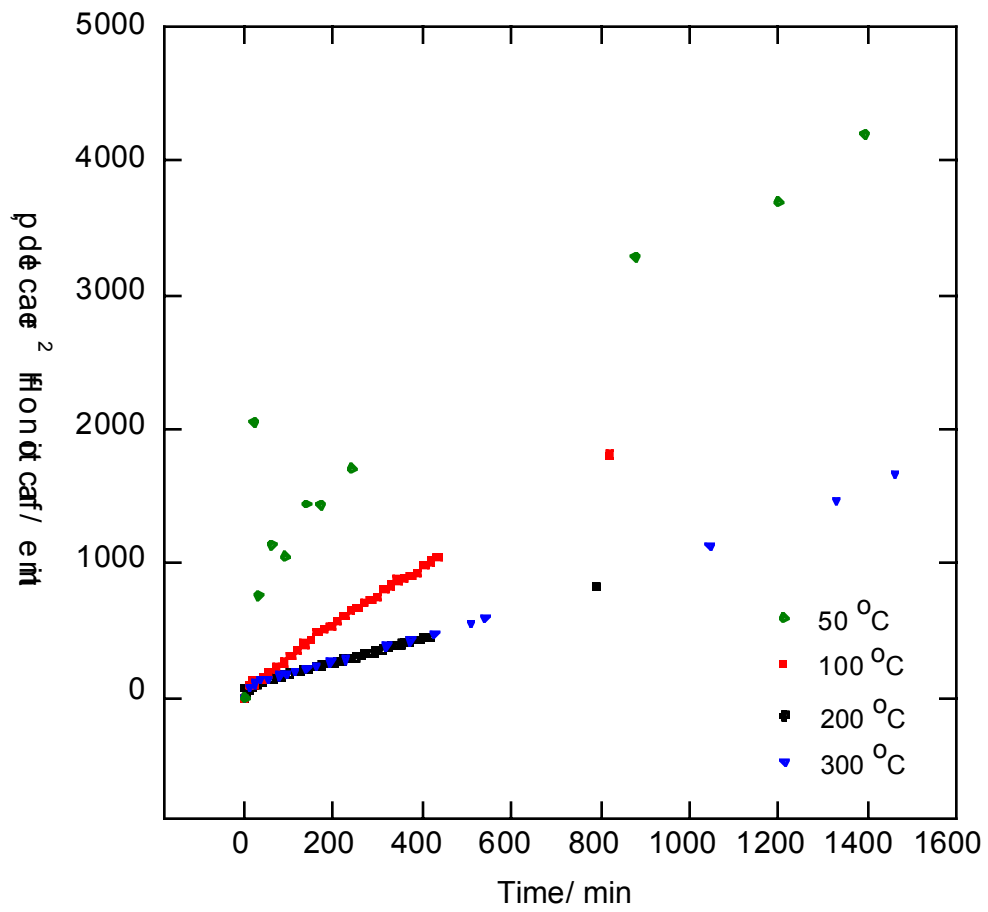


Figure 6. Plots of t/p versus time for the pure oxides.

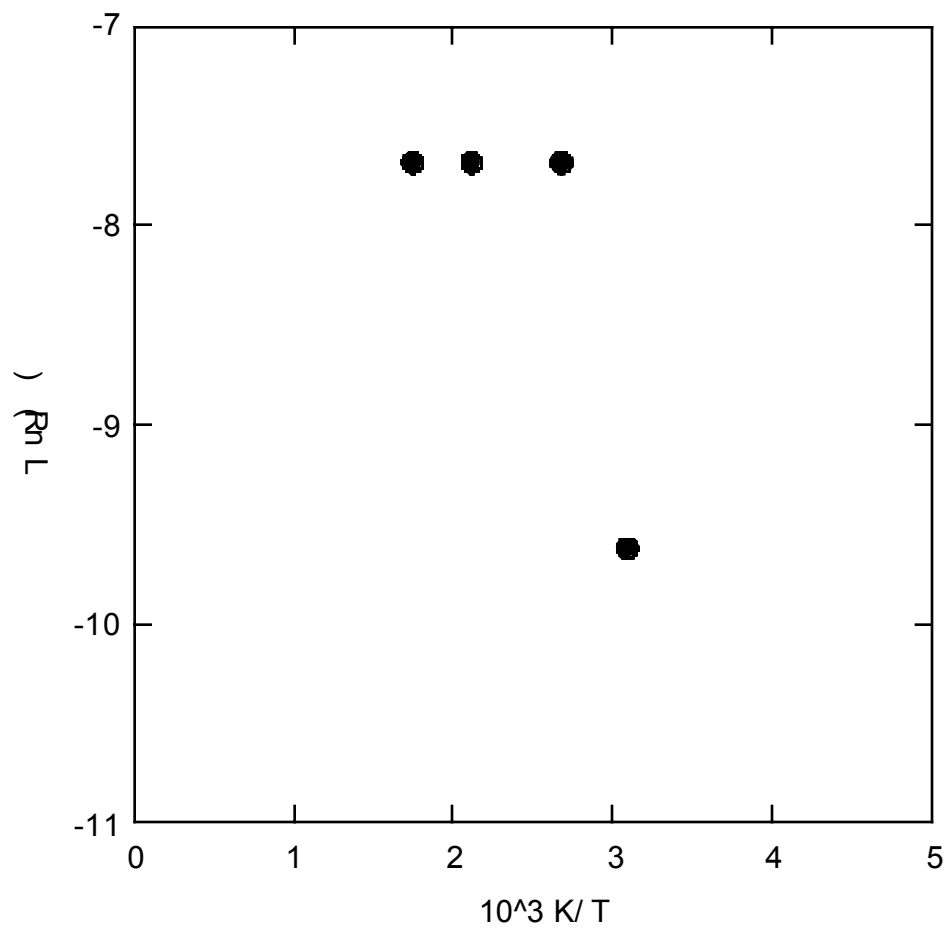


Figure 7. Dependence of $\ln R$ on the reciprocal temperature in Kelvin for the hydrogen-oxygen recombination reaction. The data are listed in Table IX.

Table I. X-ray Diffraction Results for Sample ARF-102-85-295.

2-Theta	d(A)	Int	I%	FWHM*
27.322	3.2614	5	4.9	0.214
28.353	3.1451	102	100.0	0.315
30.087	2.9677	6	5.9	0.360
31.611	2.8280	37	36.3	0.206
33.139	2.7010	25	24.5	0.417
35.507	2.5262	13	12.7	0.308
40.498	2.2256	30	29.4	0.287
43.134	2.0955	5	4.9	0.150
45.400	1.9960	15	14.7	0.241
47.468	1.9138	20	19.6	0.327
50.127	1.8183	5	4.9	0.100
52.704	1.7353	2	2.0	0.067
56.331	1.6319	28	27.5	0.406
57.040	1.6133	1	1.0	0.100
58.341	1.5804	5	4.9	0.110
58.679	1.5721	10	9.8	0.818
59.041	1.5633	8	7.8	0.514
62.681	1.4810	7	6.9	0.262
66.320	1.4083	9	8.8	0.338
73.783	1.2832	2	2.0	0.164
75.263	1.2616	6	5.9	0.300
76.833	1.2396	10	9.8	0.818
78.217	1.2211	3	2.9	0.084
79.133	1.2093	5	4.9	0.409
83.584	1.1558	2	2.0	0.078
88.693	1.1020	5	4.9	0.090
89.210	1.0969	5	4.9	0.250
89.604	1.0931	1	1.0	0.045
95.314	1.0422	9	8.8	0.506
102.891	0.9850	2	2.0	0.069
108.604	0.9485	2	2.0	0.067
110.358	0.9383	6	5.9	0.089
115.328	0.9117	3	2.9	0.104
118.774	0.8950	1	1.0	0.082
122.789	0.8774	3	2.9	0.077
129.102	0.8531	3	2.9	0.245

Calculated lattice constant for PuO₂: 5.4081(3)

Calculated O/Pu: 1.967

* Full Width at Half Maximum

Table II. Measured Total Pressures and Calculated Initial Total Moles of Gas for each Experiment

Experiment	Temp/ °C	Total Pressure at Room Temp/ Torr	Total Number of Moles of Gas at Room Temp.
Data for the Pure Oxide:			
PVT2113-1-50-p	50	552.61	1.051e-3
PVT2113-1-100-p	100	517.23	9.839e-4
PVT2120-1-200-p	200	462.64	8.801e-4
PVT2120-1-300-p	300	420.35	7.998e-4
Data for the Impure Oxide:			
PVT2120-1-200-arf	200	462.64	8.801e-4
PVT2113-1-300-arf	300	420.35	7.998e-4

Table III. Summary of the Initial and Final Gas Compositions Determined By Mass Spectrometry for Experiments PVT2120-1-200-P2 and PVT2120-1-300-P.

Experiment	Species	Initial Gas Composition/moles	Final Gas Composition/moles	Change in the Gas Composition/moles
Data for the Pure Oxide at 200 °C:				
PVT2120-1-200-P2	Hydrogen	1.78e-5	1.94e-7	-1.77e-5
	Water	0.00	2.45e-7	2.45e-7
	Nitrogen	6.88e-4	6.91e-4	3.08e-6
	Oxygen	1.74e-4	1.64e-4	-1.06e-5
	Argon	2.69e-7	1.31e-7	-1.38e-7
	Carbon	7.20e-8	1.35e-6	1.28e-6
	Dioxide			
Data for the Pure Oxide at 300 °C:				
PVT2120-1-300-P	Hydrogen	1.62e-5	1.40e-7	-1.61e-5
	Water	0.00	3.06e-7	3.06e-7
	Nitrogen	6.25e-4	6.27e-4	2.08e-6
	Oxygen	1.58e-4	1.48e-4	-9.85e-6
	Argon	2.44e-7	9.16e-8	-1.53e-7
	Carbon	6.54e-8	1.32e-6	1.25e-6
	Dioxide			

Table IV. Summary of the Kinetic Data for the Pure Oxide at 50 °C

Pressure/ Torr	Time/ min	Delta P/Torr	H ₂ consumed/ Torr	O ₂ consumed/ Torr	Moles of H ₂	Moles of O ₂	c/c ₀	Fraction of H ₂ Reacted, p	t/p
581.10	0.00	0.00	0.00	0.00	2.13e-5	2.08e-4	1.00	0.00	0.00
581.38	1.00	-0.28	–	–	–	–	–	–	–
581.10	3.00	0.00	0.00	0.00	2.13e-5	2.08e-4	1.00	0.00	0.00
581.28	12.00	-0.18	–	–	–	–	–	–	–
580.92	22.00	0.18	0.12	0.06	2.11e-5	2.08e-4	0.99	0.01	2054.18
580.40	32.00	0.70	0.47	0.23	2.04e-5	2.08e-4	0.96	0.04	768.32
580.22	60.00	0.88	0.59	0.29	2.02e-5	2.08e-4	0.95	0.05	1145.92
579.66	90.00	1.44	0.96	0.48	1.95e-5	2.07e-4	0.91	0.09	1050.43
579.47	140.00	1.63	1.09	0.54	1.92e-5	2.07e-4	0.90	0.10	1443.54
579.12	170.00	1.98	1.32	0.66	1.88e-5	2.07e-4	0.88	0.12	1443.02
578.74	240.00	2.36	1.57	0.79	1.83e-5	2.07e-4	0.86	0.14	1709.18
576.60	880.00	4.50	3.00	1.50	1.56e-5	2.05e-4	0.73	0.27	3286.68
575.65	1200.00	5.45	3.63	1.82	1.44e-5	2.05e-4	0.68	0.32	3700.60
575.52	1395.00	5.58	3.72	1.86	1.42e-5	2.05e-4	0.67	0.33	4201.72
572.82	5370.00	8.28	5.52	2.76	1.08e-5	2.03e-4	0.51	0.49	10900.12
571.76	6780.00	9.34	6.23	3.11	9.47e-6	2.02e-4	0.44	0.56	12200.30
571.77	8505.00	9.33	6.22	3.11	9.48e-6	2.02e-4	0.44	0.56	15320.76

Table V. Summary of the Kinetic Data for the Pure Oxide at 100 °C

Pressure/ Torr	Time/ min	Delta P/Torr	H ₂ consumed/ Torr	O ₂ consumed/ Torr	Moles of H ₂	Moles of O ₂	c/c ₀	Fraction of H ₂ Reacted, p	t/p
581.50	0.00	0.00	0.00	0.00	2.00e-5	1.95e-4	1.00	0.00	0.00
579.88	9.00	1.62	1.08	0.54	1.79e-5	1.94e-4	0.90	0.10	87.40
579.09	19.00	2.41	1.61	0.80	1.69e-5	1.93e-4	0.85	0.15	124.02
578.26	21.00	3.24	2.16	1.08	1.58e-5	1.93e-4	0.79	0.21	101.96
577.51	34.00	3.99	2.66	1.33	1.49e-5	1.92e-4	0.75	0.25	134.05
576.86	39.00	4.64	3.09	1.55	1.41e-5	1.92e-4	0.71	0.29	132.22
577.14	44.00	4.36	2.91	1.45	1.44e-5	1.92e-4	0.72	0.28	158.75
576.86	54.00	4.64	3.09	1.55	1.41e-5	1.92e-4	0.71	0.29	183.08
576.56	69.00	4.94	3.29	1.65	1.37e-5	1.92e-4	0.69	0.31	219.73
576.16	89.00	5.34	3.56	1.78	1.32e-5	1.91e-4	0.66	0.34	262.18
576.24	104.00	5.26	3.51	1.75	1.33e-5	1.91e-4	0.67	0.33	311.03
576.26	119.00	5.24	3.49	1.75	1.33e-5	1.91e-4	0.67	0.33	357.25
576.24	134.00	5.26	3.51	1.75	1.33e-5	1.91e-4	0.67	0.33	400.75
576.01	149.00	5.49	3.66	1.83	1.30e-5	1.91e-4	0.65	0.35	426.95
576.21	164.00	5.29	3.53	1.76	1.32e-5	1.91e-4	0.66	0.34	487.69
576.03	179.00	5.47	3.65	1.82	1.30e-5	1.91e-4	0.65	0.35	514.78
575.78	194.00	5.72	3.81	1.91	1.27e-5	1.91e-4	0.64	0.36	533.54
575.76	209.00	5.74	3.83	1.91	1.27e-5	1.91e-4	0.64	0.36	572.79
575.69	224.00	5.81	3.87	1.94	1.26e-5	1.91e-4	0.63	0.37	606.50
575.71	239.00	5.79	3.86	1.93	1.26e-5	1.91e-4	0.63	0.37	649.35
575.51	254.00	5.99	3.99	2.00	1.24e-5	1.91e-4	0.62	0.38	667.06
575.46	269.00	6.04	4.03	2.01	1.23e-5	1.91e-4	0.62	0.38	700.61
575.35	284.00	6.15	4.10	2.05	1.22e-5	1.91e-4	0.61	0.39	726.44
575.25	299.00	6.25	4.17	2.08	1.20e-5	1.91e-4	0.60	0.40	752.57
575.34	314.00	6.16	4.11	2.05	1.21e-5	1.91e-4	0.61	0.39	801.88
575.33	329.00	6.17	4.11	2.06	1.21e-5	1.91e-4	0.61	0.39	838.82
575.32	344.00	6.18	4.12	2.06	1.21e-5	1.91e-4	0.61	0.39	875.65
575.15	359.00	6.35	4.23	2.12	1.19e-5	1.91e-4	0.60	0.40	889.36
574.99	374.00	6.51	4.34	2.17	1.17e-5	1.91e-4	0.59	0.41	903.75
574.95	389.00	6.55	4.37	2.18	1.16e-5	1.91e-4	0.58	0.42	934.26
575.06	404.00	6.44	4.29	2.15	1.18e-5	1.91e-4	0.59	0.41	986.86
575.01	419.00	6.49	4.33	2.16	1.17e-5	1.91e-4	0.59	0.41	1015.61
574.98	434.00	6.52	4.35	2.17	1.17e-5	1.91e-4	0.59	0.41	1047.13
574.39	819.00	7.11	4.74	2.37	1.09e-5	1.90e-4	0.55	0.45	1812.06

Table VI. Summary of the Kinetic Data for the Pure Oxide at 200 °C

Pressure/ Torr	Time/ min	Delta P/Torr	H ₂ consumed /Torr	O ₂ consumed /Torr	Moles of H ₂	Moles of O ₂	c/c ₀	Fraction of H ₂ Reacted, p	t/p
581.60	0.00	0.00	0.00	0.00	1.78e-5	1.74e-4	1.00	0.00	0.00
581.20	2.00	0.40	0.27	0.13	1.73e-5	1.74e-4	0.97	0.03	70.35
580.00	5.00	1.60	1.07	0.53	1.58e-5	1.73e-4	0.89	0.11	43.97
579.00	10.00	2.60	1.73	0.87	1.45e-5	1.73e-4	0.82	0.18	54.12
578.30	15.00	3.30	2.20	1.10	1.37e-5	1.72e-4	0.77	0.23	63.96
577.80	27.00	3.80	2.53	1.27	1.30e-5	1.72e-4	0.73	0.27	99.98
576.90	40.00	4.70	3.13	1.57	1.19e-5	1.71e-4	0.67	0.33	119.75
575.80	55.00	5.80	3.87	1.93	1.05e-5	1.71e-4	0.59	0.41	133.43
574.80	70.00	6.80	4.53	2.27	9.22e-6	1.70e-4	0.52	0.48	144.85
574.20	85.00	7.40	4.93	2.47	8.46e-6	1.70e-4	0.47	0.53	161.62
573.70	100.00	7.90	5.27	2.63	7.83e-6	1.69e-4	0.44	0.56	178.11
573.10	115.00	8.50	5.67	2.83	7.07e-6	1.69e-4	0.40	0.60	190.37
572.70	130.00	8.90	5.93	2.97	6.56e-6	1.69e-4	0.37	0.63	205.53
572.00	145.00	9.60	6.40	3.20	5.67e-6	1.68e-4	0.32	0.68	212.53
571.80	160.00	9.80	6.53	3.27	5.42e-6	1.68e-4	0.30	0.70	229.73
571.50	175.00	10.10	6.73	3.37	5.04e-6	1.68e-4	0.28	0.72	243.80
570.90	190.00	10.70	7.13	3.57	4.28e-6	1.67e-4	0.24	0.76	249.86
570.60	205.00	11.00	7.33	3.67	3.89e-6	1.67e-4	0.22	0.78	262.23
570.50	220.00	11.10	7.40	3.70	3.77e-6	1.67e-4	0.21	0.79	278.88
570.20	235.00	11.40	7.60	3.80	3.39e-6	1.67e-4	0.19	0.81	290.06
569.90	250.00	11.70	7.80	3.90	3.01e-6	1.67e-4	0.17	0.83	300.66
569.80	265.00	11.80	7.87	3.93	2.88e-6	1.67e-4	0.16	0.84	316.00
569.70	280.00	11.90	7.93	3.97	2.75e-6	1.67e-4	0.15	0.85	331.08
569.60	295.00	12.00	8.00	4.00	2.63e-6	1.67e-4	0.15	0.85	345.91

Table VI. Summary of the Kinetic Data for the Pure Oxide at 200 °C

Pressure/ Torr	Time/ min	Delta P/Torr	H ₂ consumed /Torr	O ₂ consumed /Torr	Moles of H ₂	Moles of O ₂	c/c _o	Fraction of H ₂ Reacted, p	t/p
569.50	310.00	12.10	8.07	4.03	2.50e-6	1.67e-4	0.14	0.86	360.49
569.40	325.00	12.20	8.13	4.07	2.37e-6	1.66e-4	0.13	0.87	374.84
569.30	340.00	12.30	8.20	4.10	2.25e-6	1.66e-4	0.13	0.87	388.95
569.20	355.00	12.40	8.27	4.13	2.12e-6	1.66e-4	0.12	0.88	402.84
569.10	370.00	12.50	8.33	4.17	1.99e-6	1.66e-4	0.11	0.89	416.50
568.90	385.00	12.70	8.47	4.23	1.74e-6	1.66e-4	0.010	0.90	426.56
568.90	400.00	12.70	8.47	4.23	1.74e-6	1.66e-4	0.010	0.90	443.18
568.60	415.00	13.00	8.67	4.33	1.36e-6	1.66e-4	0.08	0.92	449.19
568.10	790.00	13.50	9.00	4.50	7.24e-7	1.66e-4	0.04	0.96	823.41

Table VII. Summary of the Kinetic Data for the Pure Oxide at 300 °C

Pressure/ Torr	Time/ min	Delta P/Torr	H ₂ consumed/ Torr	O ₂ consumed/ Torr	Moles of H ₂	Moles of O ₂	c/c ₀	Fraction of H ₂ Reacted, p	t/p
581.10	0.00	0.00	0.00	0.00	1.62e-5	1.58e-4	1.00	0.00	0.00
579.30	12.00	1.80	1.20	0.60	1.39e-5	1.57e-4	0.86	0.14	85.23
578.40	23.00	2.70	1.80	0.90	1.28e-5	1.57e-4	0.79	0.21	108.91
577.80	34.00	3.30	2.20	1.10	1.20e-5	1.56e-4	0.74	0.26	131.72
576.60	52.00	4.50	3.00	1.50	1.05e-5	1.55e-4	0.65	0.35	147.73
575.20	79.00	5.90	3.93	1.97	8.73e-6	1.55e-4	0.54	0.46	171.18
574.50	92.00	6.60	4.40	2.20	7.84e-6	1.54e-4	0.48	0.52	178.21
573.80	114.00	7.30	4.87	2.43	6.96e-6	1.54e-4	0.43	0.57	199.65
572.80	140.00	8.30	5.53	2.77	5.69e-6	1.53e-4	0.35	0.65	215.64
572.40	161.00	8.70	5.80	2.90	5.18e-6	1.53e-4	0.32	0.68	236.59
571.90	194.00	9.20	6.13	3.07	4.55e-6	1.52e-4	0.28	0.72	269.59
571.10	226.00	10.00	6.67	3.33	3.53e-6	1.52e-4	0.22	0.78	288.93
570.60	319.00	10.50	7.00	3.50	2.90e-6	1.52e-4	0.18	0.82	388.41
570.00	373.00	11.10	7.40	3.70	2.14e-6	1.51e-4	0.13	0.87	429.61
569.70	427.00	11.40	7.60	3.80	1.76e-6	1.51e-4	0.11	0.89	478.86
569.50	509.00	11.60	7.73	3.87	1.50e-6	1.51e-4	0.09	0.91	560.98
569.40	541.00	11.70	7.80	3.90	1.38e-6	1.51e-4	0.08	0.92	591.15
569.30	1046.00	11.80	7.87	3.93	1.25e-6	1.51e-4	0.08	0.92	1133.27
569.60	1331.00	11.50	7.67	3.83	1.63e-6	1.51e-4	0.10	0.90	1479.67
569.90	1461.00	11.20	7.47	3.73	2.01e-6	1.51e-4	0.12	0.88	1667.69

Table VIII. Summary of the Kinetic Data for the ImPure Oxide at 200 and 300 °C

Pressure/ Torr	Time/ min	Delta P/Torr	H ₂ consumed/Torr	O ₂ consumed/Torr	Moles of H ₂	Moles of O ₂
Data collected at 200 °C:						
581.70	0.00	0.00	0.00	0.00	1.78e-5	1.74e-4
579.00	100.00	2.70	1.80	0.90	1.44e-5	1.73e-4
578.00	150.00	3.70	2.47	1.23	1.32e-5	1.72e-4
577.00	220.00	4.70	3.13	1.57	1.19e-5	1.71e-4
576.00	400.00	5.70	3.80	1.90	1.06e-5	1.71e-4
580.30	57.00	1.40	0.93	0.47	1.61e-5	1.73e-4
576.50	300.00	5.20	3.47	1.73	1.13e-5	1.71e-4
Data collected at 300 °C:						
581.60	0.00	0.00	0.00	0.00	1.62e-5	1.58e-4
580.00	37.00	1.60	1.07	0.53	1.42e-5	1.57e-4
579.00	57.00	2.60	1.73	0.87	1.29e-5	1.57e-4
578.00	90.00	3.60	2.40	1.20	1.16e-5	1.56e-4
577.00	100.00	4.60	3.07	1.53	1.04e-5	1.55e-4
576.00	149.00	5.60	3.73	1.87	9.11e-6	1.55e-4
575.00	200.00	6.60	4.40	2.20	7.84e-6	1.54e-4
574.00	300.00	7.60	5.07	2.53	6.58e-6	1.53e-4
573.00	400.00	8.60	5.73	2.87	5.31e-6	1.53e-4

Table IX. Calculated Rates of Water Formation for the Pure and Impure Oxides

Description	Time/min	moles H ₂	Temp./°C	moles H ₂ / min	moles H ₂ O/m ² *day	10 ³ K/ T	ln (Rate)
Data for the Pure Oxide:							
100 °C	0.00	2.00e-5					
	9.00	1.79e-5	300	1.62e-7	4.59e-4	1.745	-7.67
	19.00	1.69e-5	200	1.62e-7	4.59e-4	2.114	-7.67
	21.00	1.58e-5	100	1.62e-7	4.59e-4	2.681	-7.67
200 °C	0.00	1.78e-5	50	2.34e-8	6.63e-5	3.096	-9.62
	2.00	1.73e-5					
	5.00	1.58e-5					
	10.00	1.45e-5	300	5.53e-8	2.63e-4	1.745	-8.24
	15.00	1.37e-5	200	2.74e-8	1.30e-4	2.114	-8.95
300 °C	27.00	1.30e-5					
	0.00	1.62e-5					
	12.00	1.39e-5					
	23.00	1.28e-5					
50 °C	34.00	1.20e-5					
	0.00	2.13e-5					
	1.00	2.17e-5					
	3.00	2.13e-5					
	12.00	2.15e-5					
	22.00	2.11e-5					
	32.00	2.04e-5					
60.00	2.02e-5						
Data for the Impure Oxide:							
200 °C	0.00	1.78e-5					
	100.00	1.44e-5					
	150.00	1.32e-5					
	220.00	1.19e-5					
300 °C	0.00	1.62e-5					
	37.00	1.42e-5					
	57.00	1.29e-5					
	90.00	1.16e-5					
	100.00	1.04e-5					